Homandberg, G. A., & Chaiken, I. M. (1980) *J. Biol. Chem. 255*, 4903.
Homandberg, G. A., Mattis, J. A., & Laskowski, M., Jr. (1978) *Biochemistry 17*, 5220–5227.
Iyer, K. S., & Acharya, A. S. (1987) *Proc. Natl. Acad. Sci. U.S.A. 84*, 7014–7018.
Jullierat, M., & Homandberg, G. A. (1981) *Int. J. Pept. Protein Res. 18*, 335–342.
Knowles, J. R. (1987) *Science 236*, 1252–1258.
Komoriya, A., Homandberg, G. A., & Chaiken, I. M. (1980) *Int. J. Pept. Protein Res. 16*, 433–439.
Kullman, W. (1985) *J. Protein Chem. 4*, 1–22.
Murphy, J., Zhang, W., Macauly, W., Fasman, G., & Merrifield, R. B. (1986) *J. Biol. Chem. 262*, 17304–17312.
Nagai, K., Perutz, M. F., & Poyart, C. (1985) *Proc. Natl. Acad. Sci. U.S.A. 82*, 7252–7255.
Nagai, K., Thorgersen, H. C., & Luisi, B. F. (1988) *Biochem. Soc. Trans. 16*, 108–110.
Offord, J. E. (1985) *Pept.: Struct. Funct., Proc. Am. Pept. Symp., 9th, 1985*, 325–334.
Offord, J. E. (1987) *Protein Eng. 1*, 151–157.
Richards, F. M., & Wychoff, H. W. (1971) *Enzymes 4*, 647.
Seetharam, R., & Acharya, A. S. (1986) *J. Cell. Biochem. 30*, 87–99.
Seetharam, R., Dean, A., Iyer, K. S., & Acharya, A. S. (1986) *Biochemistry 25*, 5949–5955.
Ward, W. H. J., & Fersht, A. R. (1988) *Biochemistry 27*, 1041–1049.
Yip, Y. K., Waks, M., & Beychok, S. (1972) *J. Biol. Chem. 248*, 7237–7244.

Resonance Raman Studies of *Escherichia coli* Sulfite Reductase Hemoprotein. 1. Siroheme Vibrational Modes†

Sanghwa Han,‡ John F. Madden,§ Ronald G. Thompson,∥ Steven H. Strauss,∥ Lewis M. Siegel,*,§ and Thomas G. Spiro‡

Department of Chemistry, Princeton University, Princeton, New Jersey 08540, Department of Biochemistry, Duke University Medical Center and Veterans Administration Hospital, Durham, North Carolina 27705, and Department of Chemistry, Colorado State University, Fort Collins, Colorado 80523

Received November 4, 1988; Revised Manuscript Received March 14, 1989

ABSTRACT: Resonance Raman (RR) spectra are reported for the hemoprotein subunit (SiR-HP) of *Escherichia coli* NADPH–sulfite reductase (EC 1.8.1.2) in various ligation and redox states. Comparison of the RR spectra of extracted siroheme and the μ-oxo Fe^{III} dimer of octaethylisobacteriochlorin with those of μ-oxo Fe^{III} octaethylchlorin dimer and μ-oxo Fe^{III} octaethylporphyrin dimer demonstrates that many siroheme bands can be correlated with established porphyrin skeletal modes. Depolarization measurements are a powerful tool in this correlation, since the 45° rotation of the C_2 symmetry axis of the isobacteriochlorin ring relative to the chlorin system results in reversal of the polarization properties (polarized vs anomalously polarized) of bands correlating with B_{1g} and B_{2g} modes of porphyrin. Various SiR-HP adducts (CO, NO, CN^-, SO_3^{2-}) show upshifted high-frequency bands, characteristic of the low-spin state and consistent with the expected core size sensitivity of the skeletal modes. Fully reduced unliganded SiR-HP (both siroheme and Fe_4S_4 cluster reduced) in liquid solution displays RR features comparable to those of high-spin ferrous porphyrins; on freezing, the RR spectrum changes, reflecting an apparent mixture of siroheme spin states. At intermediate reduction levels in solution a RR species is observed whose high-frequency bands are upshifted relative to oxidized and fully reduced SiR-HP. This spectrum, thought to arise from the "one-electron" state of SiR-HP (siroheme reduced, cluster oxidized), may be due to $S = 1$ Fe^{II} siroheme.

Escherichia coli NADPH–sulfite reductase (EC 1.8.1.2) is a multimeric hemoflavoprotein that catalyzes the six-electron reduction of sulfite to sulfide (Siegel et al., 1973, 1982; Janick et al., 1983). The hemoprotein subunit of the enzyme (SiR-HP), which contains the site of sulfite binding, possesses a novel catalytic center composed of siroheme (Murphy et al., 1973), an iron isobacteriochlorin (see Figure 1), closely interacting with a Fe_4S_4 cluster (Janick & Siegel, 1983). Interaction of the two centers may be of functional significance in facilitating the rapid transfer of multiple reducing equivalents to the bound substrate. The existence of a chemical linkage between the siroheme and cluster is strikingly manifested in the form of magnetic exchange coupling between the two prosthetic groups, which on the basis of Mössbauer (Christner et al., 1981,) and electron paramagnetic resonance spectroscopy (EPR) (Janick & Siegel, 1982) has been shown to persist in various redox states of the enzyme, both in the presence and in the absence of exogenous ligands. The detailed structural basis for the interaction, however, remains to be determined. A proposed model (Janick & Siegel, 1982) (see Figure 2) envisions a bridged structure in which one of the

† This work was supported by Grant GM 13498 (T.G.S.), Grant GM 31554 (S.H.S.), and Grant GM 32210 (L.M.S.) from the National Institutes of Health and by Project Grant 7875-01 from the Veterans Administration (L.M.S.). J.F.M. is a fellow of the Medical Scientist Training Program at Duke University.
‡ Princeton University.
§ Duke University Medical Center and Veterans Administration Hospital.
∥ Colorado State University.

0006-2960/89/0428-5461$01.50/0

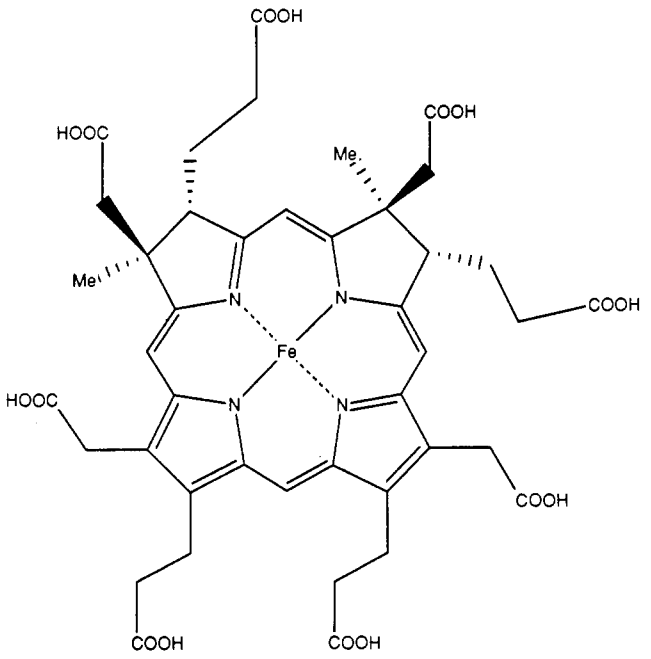

FIGURE 1: Structural diagram of siroheme.

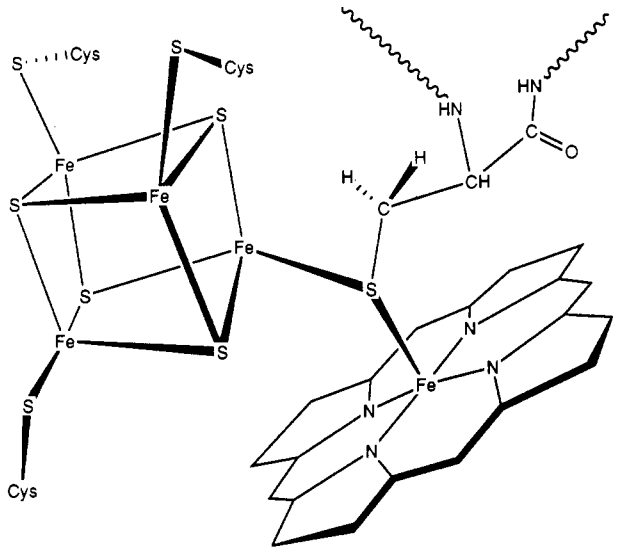

FIGURE 2: Proposed model of the active site of SiR-HP (Janick & Siegel, 1982).

Fe_4S_4 corner cysteinyl ligands simultaneously coordinates axially to the siroheme iron. The crystallographic structure of the active site (McRee et al., 1986), while compatible with this model, currently lacks sufficient resolution to unambiguously identify such a bridging ligand. The X-ray data show a 4.4-Å separation of the siroheme iron from the nearest cluster iron and the presence of electron density between these metal sites, which is consistent with a bridging sulfur or oxygen atom. In addition, direct electronic overlap between the siroheme periphery and a cubane sulfur at one corner of the cluster is possible since the two prosthetic groups appear from the electron density map to be in van der Waals contact.

In SiR-HP as isolated (SiR-HP^0), the siroheme is known to be in the high-spin ferric state (Janick & Siegel, 1982) and is thought to be five-coordinate (Cline et al., 1985). The Fe_4S_4 cluster is in the +2 (diamagnetic) state. In the absence of exogenous ligands, the enzyme can be successively reduced in two one-electron steps (Janick & Siegel, 1982). The first reducing equivalent is accommodated by the iron of the siroheme, which has been suggested on the basis of Mössbauer studies (Christner et al., 1983) to take up the unusual intermediate-spin ($S = 1$) ferrous state. The second reducing equivalent is accepted by the cluster, yielding fully reduced enzyme, which normally consists of a mixture of at least two EPR-distinguishable species (Janick & Siegel, 1982). The reduced enzyme reacts rapidly with a number of strong-field heme ligands (e.g., CN^-, CO) to yield stable adducts containing low-spin siroheme (Janick & Siegel, 1983). The reduced enzyme also reacts with its substrates, SO_3^{2-} and NO_2^-, and in the absence of sufficient reducing equivalents to complete turnover retains substrate in an enzyme-bound form (Janick et al., 1983).

Resonance Raman (RR) spectroscopy provides a sensitive probe of structural influences in and around protein-bound heme (Spiro, 1985) as well as iron-sulfur clusters (Spiro et al., 1988). Knowledge of hydroporphyrin vibrational structure, while far from complete, has advanced rapidly in recent years. RR studies of model chlorins (Ozaki et al., 1979, 1986a,b; Andersson et al., 1985, 1986) and corphins (Shelnutt, 1987) and of chlorin-containing proteins including sulfmyoglobin (Andersson et al., 1984), myeloperoxidase (Sibbett & Hurst, 1984; Babcock et al., 1985), bovine spleen green hemoprotein (Babcock et al., 1985), and *Pseudomonas aeruginosa* heme d_1 (an oxoisobacteriochlorin) (Cotton et al., 1981; Ondrias et al., 1982) have now appeared, and the consequences of the lowering of the symmetry resulting from ring reduction on the RR spectral characteristics of hydroporphyrins have been discussed. Although no model studies reporting on the RR of the isobacteriochlorin macrocycle have been previously available, Ondrias et al. (1985) have reported high-frequency spectra of the siroheme of spinach ferredoxin–nitrite reductase using Soret excitation. They noted a number of differences from chlorin and porphyrin spectra that could be rationalized on the basis of symmetry lowering and bond-order reductions in the siroheme. In this paper we report the results of RR investigations of the oxidized and reduced states of SiR-HP obtained in the absence and presence of added ligands, both in solution and in the frozen state. High-quality spectra of the siroheme moiety have been obtained across the entire Raman spectral range by using Soret and Q-band excitation and are compared with the spectrum of a model isobacteriochlorin and the extracted siroheme. Succeeding papers will be concerned with Fe_4S_4 cluster Raman spectrum, which has been identified by using ^{34}S-labeled SiR-HP, and with bound-ligand vibrations in various complexes of SiR-HP.

Experimental Procedures

Hemoprotein Subunit and Model Porphyrin Complexes. The hemoprotein subunit of *E. coli* NADPH–sulfite reductase was prepared according to the method of Siegel and Davis (1974) with minor modifications. The SiR-HP was further purified by chromatography on phenyl-Sepharose CL4B (Pharmacia) to remove the small amount (5–10%) of low-spin hemoprotein that is observed in the DEAE-cellulose eluate. The protein samples had A_{280}/A_{387} between 1.65 and 1.75 in 0.1 M potassium phosphate and 100 μM EDTA, pH 7.7, the standard buffer used in this work. The concentration of SiR-HP was determined spectrophotometrically by using $\epsilon_{591} = 18\,100\ M^{-1}\ cm^{-1}$ (Janick et al., 1983).

$[Fe(OEP)]_2O$ (OEP = octaethylporphyrin) was purchased from Midcentury (Posen, IL) and used without further purification. $[Fe(OEC)]_2O$ and $[Fe(OEiBC]_2O$ (OEC = octaethylchlorin; OEiBC = octaethylisobacteriochlorin) were synthesized as previously described (Stoltzenberg et al., 1981). The μ-oxo dimers were dissolved in dichloromethane for Raman spectroscopy.

Cr^{II}(EDTA) Reductant Solutions. Sodium dithionite is an effective reductant for SiR-HP when the enzyme is stably complexed to heme ligands that block substrate binding and turnover. However, it is inappropriate for the reduction of SiR-HP as isolated because the product of the reaction, sulfite, is a substrate for the enzyme. Reduced methylviologen is an effective reductant for SiR-HP, but its significant RR enhancement was found to obscure the enzyme spectrum. The deazaflavin/EDTA photoreduction system extensively used in the previous EPR and Mössbauer studies (Massey & Hemmerich, 1978) would be a convenient method for the preparation of reduced samples were it not for the problem of fluorescence from deazaflavin. We noted that Cr^{II}(EDTA) had been successfully employed in the reduction of Fe_4S_4 analogue complexes (Tsai et al., 1985; Henderson & Sykes, 1980) which had even lower redox potentials than the cluster in SiR-HP. Moreover, it has minimal optical absorbance in both its reduced and oxidized forms and no fluorescence. Optical and EPR spectra of samples of SiR-HP reduced with excess Cr^{II}(EDTA) were found to display the same features as the enzyme fully reduced by deazaflavin/EDTA system. Upon reoxidation in air, the spectral features of native SiR-HP are regained after Cr^{II}(EDTA) treatment. No irreversible binding of Cr to the enzyme was detected by atomic absorption analysis of SiR-HP dialyzed after Cr^{II}(EDTA) treatment. SiR-HP reduced with a 20-fold excess of Cr^{II}(EDTA) and reoxidized displayed unaltered V_{max} and K_m for sulfite in the methylviologen–sulfite assay (Siegel & Davis, 1974) compared with untreated enzyme. Control experiments showed that neither the reduced nor the oxidized Cr(EDTA) made any significant contribution to the RR spectrum of the enzyme at the concentrations used.

The Cr^{II}(EDTA) reductant was prepared as follows (Tsai et al., 1985). All solutions were thoroughly purged with inert gas. Chromous chloride (99% Aldrich) was dissolved to 0.5 M in 0.5 N HCl, and 300 μL of this solution was added to 750 μL of 0.2 M EDTA, pH 5.1. Immediately after mixing, an amount of this solution sufficient to provide the desired final Cr(EDTA) concentration (2–30 mM, depending on the experiment) was transferred to a second tube containing 3.0 mL of 0.1 M Tris-HCl, pH 8.5. In cases where chloride was undesirable, a solution of $CrSO_4$ at 0.5 M was prepared by dissolving the appropriate amount of Cr metal (99.9%, 325-mesh powder, Johnson-Matthey Aesar) in 1.5 N H_2SO_4 under gentle heating; this was used in place of the $CrCl_2$ solution, and Tris–SO_4 was substituted for Tris-HCl. Solutions of chromous ion and of Cr^{II}(EDTA) are extremely air sensitive, and some contamination of stock solutions by the chromic species was routinely noted; therefore, the reductant was always used within a few minutes of preparation. The total chromium concentration was determined by dilution of the stock solution into air-saturated 0.25 M sodium acetate, pH 4.0, on the basis of the ϵ_{542} for Cr^{III}(EDTA) of 201 M^{-1} cm^{-1} (den Boef et al., 1960).

Sample Preparation. Solutions containing SiR-HP in standard buffer were concentrated to 200–1200 μM by ultrafiltration. The preparation of ligand complexes of SiR-HP requires prior reduction of the enzyme, due to the slow rate of reaction of oxidized SiR-HP with exogenous ligands (Rueger & Siegel, 1976). Samples to be reduced were deoxygenated by at least five cycles of evacuation, argon flush, and shaking. Reduction was carried out under inert atmosphere by adding the specified amount of freshly prepared Cr^{II}(EDTA) solution. Further details of sample preparation are provided in the legends to the appropriate figure. Samples for room temperature RR spectroscopy were prepared in standard 5 mm diameter NMR tubes. Optical spectra were obtained directly on the NMR tube samples by using either a Perkin-Elmer Lambda 9 UV–Vis–NIR spectrophotometer or Hewlett-Packard Model 8452A diode array spectrophotometer. Samples for the frozen-state RR spectroscopy were prepared in microvials, and diluted aliquots were used to check the optical spectrum. The sample was then transferred in an anaerobic glovebox into the sample cup of a specially constructed Raman cell (Czernuszewicz & Johnson, 1983), which incorporates an air-tight sample chamber coupled to a liquid N_2 Dewar via a copper cold-finger. The cell was sealed within the glovebox, and the sample was frozen under the entrapped glovebox atmosphere.

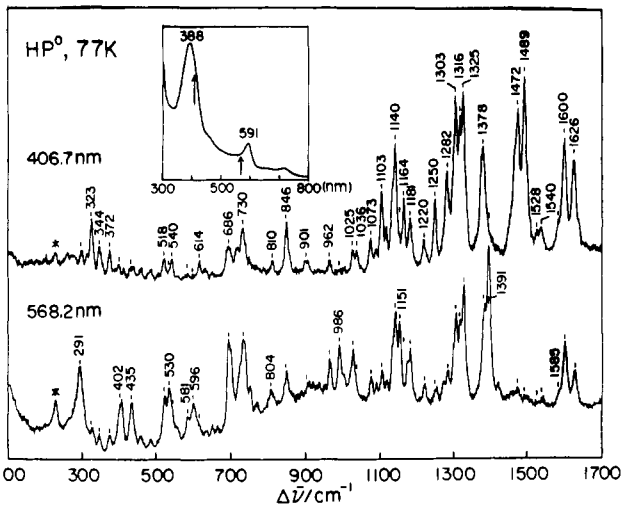

FIGURE 3: RR spectra of SiR-HP^0 (811 μM) at 77 K obtained with 406.7- and 568.2-nm excitation. Instrumental conditions (Spex 1402): power, 50 mW (406.7 nm), 80 mW (568.2 nm); slit, 7 cm^{-1}; scan increment, 1 cm^{-1}; acquisition time, 2 s/point.

RR Spectroscopy. Excitation lines were provided by a Spectra Physics Model 171 Kr^+ laser using 135° backscattering geometry. The laser power was typcially 50 mW (406.7 nm) to 80 mW (568.2 nm) at the sample. The scattered light was dispersed by a Spex 1402 double monochromator equipped with a cooled RCA 31034A photomultiplier tube and an Ortec 9315 photon counting system under the control of a DEC MINC II microcomputer. In some cases an alternate system was used that incorporated an optical multichannel analyzer (OMA) consisting of a Princeton Applied Research Model 1421 intensified silicon photodiode array detector and Model 1218 solid-state detector controller coupled to a Spex 1877 Triplemate spectrometer equipped with a grating of 2400 grooves/mm. The advantage of this instrument was the rapidity with which spectra could be collected, although the resolution was lower than that of the scanning instrument. The instrument used is specified in the figure caption as "Spex 1402" for scanning spectrometer or "Spex 1877" for the OMA system.

Results and Discussion

Oxidized SiR-HP. Figure 3 shows RR spectra of the oxidized sulfite reductase hemoprotein, SiR-HP^0, obtained with 406.7- and 568.2-nm excitation. These wavelengths were chosen to be in resonance with the two major absorption bands, Soret and Q, of the siroheme (see Figure 3, inset, absorption spectrum) centered at 387 and 591 nm, respectively. The RR spectra show low backgrounds and are richly detailed with numerous bands, ranging from 291 to 1624 cm^{-1}, which can be attributed to vibrational modes of the siroheme. The

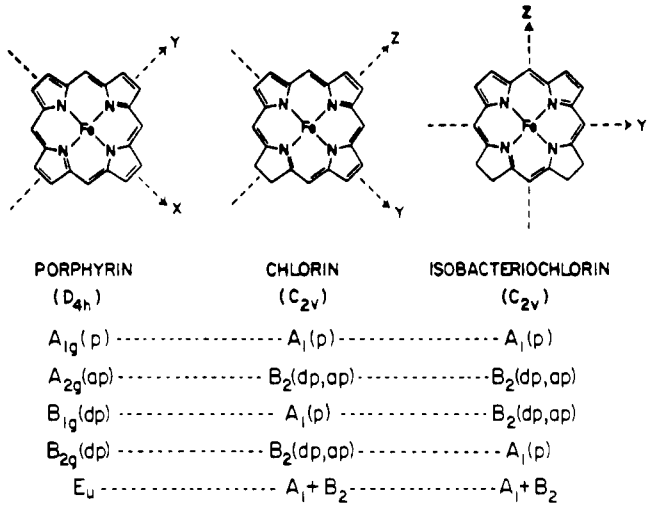

FIGURE 4: Symmetry relationships for porphyrins, chlorins, and isobacteriochlorins in their idealized D_{4h} and C_{2v} point groups.

Soret-excited spectrum contains bands ranging from polarized (p, $\rho < {}^3/_4$) to depolarized (dp, $\rho = {}^3/_4$) to anomalously polarized (ap, $\rho > {}^3/_4$). The broad, complex band around 1480 cm^{-1} gives particularly strong enhancement. A group of at least three extremely strong modes, centered at 1315 cm^{-1}, is a novel feature of the siroheme spectra in SiR-HP^0. Under Soret excitation, both sets of strong bands actually exceed in intensity the presumptive analogue of the porphyrin "oxidation-state marker" band, which is observed at 1378 cm^{-1}. As previously noted by Ondrias et al. (1985) in their spectra of nitrite reductase, unusually strong enhancement is noted for a number of modes in the 1100–1200-cm^{-1} region, while in the spectral range from 1500 to 1600 cm^{-1} few strong bands are observed, in contrast to the spectra of porphyrins and chlorins. Marked alteration in the enhancement pattern is seen for Soret, as compared with Q-band, excitation; several modes, chiefly high-frequency polarized bands (e.g., 1489, 1472, 1282, 1250, 1164, 1103, 323 cm^{-1}), are very weak or absent with 568.2-nm excitation, while others, mainly in the low-frequency region (e.g., 1391, 1151, 986, 804, 596, 581, 530, 435, 402, 291 cm^{-1}), appear only with 568.2-nm excitation.

These spectra are substantially more complex than those seen for metalloporphyrins (Spiro & Li, 1988). The increase in the number of bands is attributable to symmetry lowering, as in metallochlorin RR spectra (Ozaki et al., 1979, 1986a; Andersson et al., 1985, 1986; Boldt et al., 1987), where similar complexity is encountered. Figure 4 shows the symmetry relationships for porphyrins, chlorins, and isobacteriochlorins in their idealized D_{4h} and C_{2v} point groups. For both chlorin and isobacteriochlorin infrared (E_u) modes become Raman active, and many more modes are totally symmetric than in porphyrins. For porphyrin, totally symmetric modes are mainly enhanced in resonance with the very strong Soret band, via A (Franck–Condon) term scattering, while enhancement in resonance with the weaker Q bands occurs mainly via B term (vibronic) scattering (X.-Y. Li and T. G. Spiro, unpublished results; Spiro, 1983) and involves non totally symmetric modes. For chlorins and isobacteriochlorins the absorption strength of the two transitions is more nearly equal, and significant A *and* B term scattering should be encountered for both electronic transitions, as experimentally verified by the strong enhancement of bands of all polarizations in both Soret- and Q-band-excited spectra reported here. The resonance enhancement patterns nevertheless differ significantly between Soret and Q-band resonance, as noted above, reflecting different shapes for the excited-state potentials. In addition, the enhancement pattern should depend on the exact excitation wavelength within the major absorption bands; due to the degeneracy lifting in isobacteriochlorins (Gouterman, 1961), differential activity is expected for the *y*- vs *z*-polarized components of the Soret and Q electronic transitions. Such effects have been noted, for example, in variable-wavelength excitation of copper chlorophyllin surface-enhanced RR spectra (Hildebrandt & Spiro, 1988) and in the spectra of nickel dihydroporphyrins (Boldt et al., 1987). For SiR-HP^0, however, the enhancement pattern of spectra obtained by using 590.0-nm excitation (not shown) was quite similar to that obtained with 568.2-nm excitation.

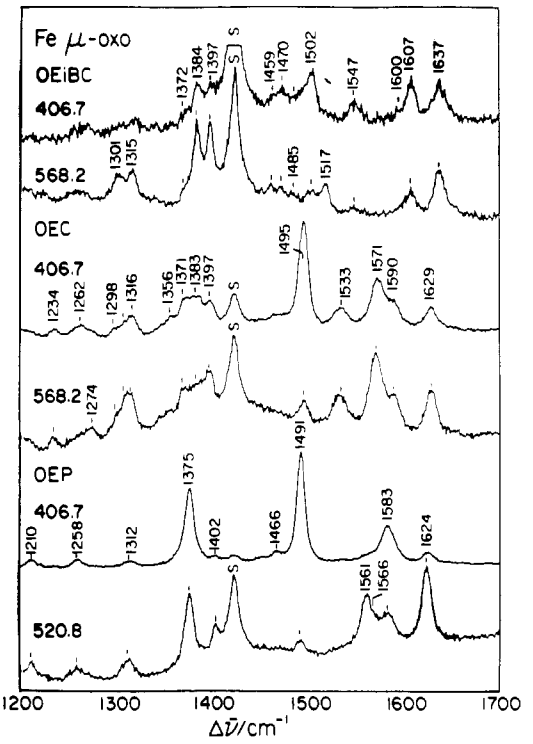

FIGURE 5: Room temperature RR spectra of μ-oxo dimers of Fe^{III} OEP, OEC, and OEiBC in CH_2Cl_2 obtained with 406.7, 520.8, and 568.2-nm excitation. The bands marked S are due to solvent. Instrumental conditions (Spex 1402): power, 70 mW (406.7 nm), 100 mW (520.8, 568.2 nm); slit, 6 cm^{-1}; scan increment, 1 cm^{-1}; acquisition time, 1–6 s/point.

Porphyrin/Isobacteriochlorin Mode Correlations. In attempting to make sense of the complex siroheme spectra, one is naturally drawn to correlations with RR spectra of metalloporphyrins, which have been thoroughly analyzed (Abe et al., 1978; Spiro & Li, 1988; X.-Y. Li, J. R. Kincaid, R. S. Czernuszewicz, P. Stein, and T. G. Spiro, unpublished results). This approach has been applied to chlorins (Ozaki et al., 1979, 1986a,b; Andersson et al., 1985, 1986; Kitagawa & Ozaki, 1987) with satisfying results. In Figure 5 the RR spectra of the μ-oxo Fe^{III} dimers of octaethylporphyrin (OEP), octaethylchlorin (OEC), and octaethylisobacteriochlorin (OEiBC) are compared. These species have the same oxidation, spin, and coordination state (five-coordinate high-spin Fe^{III}) and the same peripheral substituents; they differ only in the nature of the tetrapyrrole ring. In Table I we have suggested correlations among the observed bands and listed the corresponding RR frequencies for SiR-HP^0 and siroheme extracted into acetone-d_6/HCl. At a minimum, the correlations provide a useful systematization of the OEiBC RR bands, using the familiar porphyrin notation system. The significance of such correlations has recently been called into question (Boldt et al., 1987) on the basis of the results of normal mode calculations on chlorins. Using the QCFF-PI electronic structure

Table I: Vibrational Assignments for Heme Bands at Room Temperature

porphyrin mode[a]			OEP[b]	OEC[b]	OEiBC[b]	siroheme	HP[0]
ν_{10}	B_{1g}	$\nu(C_\alpha C_m)$	1624 dp	1629 p	1637 ap	1631	1622 ap
ν_2	A_{1g}	$\nu(C_\beta C_\beta)$	1583 p	1590 p	1607 p	1599	1596 p
ν_{19}	A_{2g}	$\nu(C_\alpha C_m)$	1566 ap[c]	1571 dp	1600	1587 (sh)	1585 dp[c]
ν_{38}	E_u	$\nu(C_\alpha C_m)$			1547	1537	1536, 1524
ν_{11}	B_{1g}	$\nu(C_\beta C_\beta)$	1561 cp[c]	1533 p	1517 ap	1514	
ν_3	A_{1g}	$\nu(C_\alpha C_m)$	1491 p	1495 p	1502 p	sh[d]	1488 p
ν_{28}	B_{2g}	$\nu(C_\alpha C_m)$	1466 dp		1485[c]	1476	1468 p
					1470	sh	1458[c]
					1459[c]	sh	1451[c]
							1421 p[c]
ν_{29}	B_{2g}	$\nu(C_\alpha C_b)$	1402 dp[c]	1397 dp	1397 p[c]	1391	1390 p[c]
ν_4	A_{1g}	$\nu(C_\alpha N)$	1375 p	1383 p	1384 p[c]	1380	1375 p
				1371 p	1372		
						1325	1324 p
ν_{21}	A_{2g}	$\delta(C_m H)$	1312 ap	1316 dp	1315 dp		1315 dp
					1301 p	1302	1303 p
				1298			1296 p[c]
							1280 p
ν_{42}	E_u	$\delta(C_m H)$		1274			1271 dp[c]
			1258 p	1262 p	1263		1249 p
ν_{13}	B_{1g}	$\delta(C_m H)$	1210 dp	1234 p		1235	1219 ap

[a] Assignments based on normal mode analysis for Ni(OEP) (Abe et al., 1978). [b] Ferric μ-oxo dimer. [c] Better estimated from Q-band-excited spectra. [d] Shoulder.

program to accommodate the expected bond-order changes, these investigators reached the conclusion that there is considerable mixing of porphyrin-derived modes in the lower symmetry environment of the chlorin macrocycle, resulting in localization of certain high-frequency modes to inequivalent regions of the dihydroporphyrin ring. Nevertheless, they found that chlorin bands could usually be meaningfully related, via their polarization and activation properties, to contributions from a small number (one to three) of porphyrin normal modes. It is certainly to be expected that the bond alterations associated with ring reduction will change the character of the isobacteriochlorin normal modes. But there is reason to think, as discussed in the succeeding paragraphs, that the correlated modes bear recognizable similarities to their porphyrin parents, despite inevitable alterations in mode composition. A more central question here is whether the mode frequencies retain similar qualitative responses to structural alterations such as spin-state change of the central metal despite the altered compositions. That this is likely to be the case is indicated by the finding that sensitivity to the macrocycle core size between high-frequency modes correlated in this manner is quite similar for porphyrin (Spiro & Li, 1988) and for chlorin (Ozaki et al., 1986a; Kitagawa & Ozaki, 1987). We will present evidence below that with an important exception similar sensitivity is retained by the isobacteriochlorin siroheme.

In formulating the correlations we make use of the symmetry relationships illustrated in Figure 4, aided by a significant difference in chlorin and isobacteriochlorin symmetry. Although both reduced ring systems fall into the C_{2v} point group, the two-fold symmetry axis (z) is rotated by 45° with respect to the tetrapyrrole frame, passing through the reduced pyrrole ring in chlorin but between the two reduced rings in isobacteriochlorin. The result is a reversal in the correlation of the porphyrin B_{1g} and B_{2g} modes, to A_1 and B_2 for chlorin, but to B_2 and A_1 for isobacteriochlorin. Modes correlating with porphyrin B_{1g} modes are polarized for chlorin but depolarized or anomalously polarized for isobacteriochlorin and vice versa for B_{2g} modes. For the same reason, mixing of porphyrin A_{2g} (anomalously polarized) derived modes, should it occur, would involve B_{2g} (or E_u) derived modes in chlorin, but B_{1g} (or E_u) derived modes in isobacteriochlorin. The highest frequency RR band nicely illustrates these relationships. This is the porphyrin ν_{10} mode, of B_{1g} symmetry and depolarized in OEP ($\rho \sim 0.8$). In OEC the highest frequency band is therefore polarized ($\rho \sim 0.3$) as expected (see Figure 4), while for OEiBC it is anomalously polarized ($\rho \geq 1.0$), in striking confirmation of the symmetry correlation and possibly suggestive of mode mixing involving the nearby porphyrin ν_{19} (A_{2g}, anomalously polarized) derived vibration. Another illustration is given by the depolarized OEP mode at 1402 cm^{-1}, which is assigned to ν_{29} (B_{2g}) and which correlates with a depolarized OEC band but a polarized OEiBC band at essentially the same frequency (both at 1397 cm^{-1}). The porphyrin A_{1g} modes remain totally symmetric (A_1) and hence polarized for both chlorin and isobacteriochlorin. This relationship can be discerned for the OEC and OEiBC bands corresponding most closely in frequency to the OEP ν_3 and ν_4 modes. These correlations gain credence from the fact that all of the porphyrin Raman modes above 1312 cm^{-1} find corresponding bands with the correct polarization in both chlorin and isobacteriochlorin spectra.

The dynamical effect of pyrrole $C_\beta C_\beta$ bond-order reduction in the reduced ring systems is anticipated to be a downshift in the frequency of modes principally involving $C_\beta C_\beta$ motion. The porphyrin ν_{11} (B_{1g}) mode mainly involves $C_\beta C_\beta$ bond stretching (Abe et al., 1978), and as expected, the correlation shows this mode decreasing strongly from OEP (1561 cm^{-1}, dp) to OEC (1533 cm^{-1}, p) to OEiBC (1517 cm^{-1}, ap). On the other hand, the band at 1607 cm^{-1} in OEiBC, which appears to be associated with the porphyrin $\nu_2(A_{1g})$ mode on the basis of its polarization and intensity properties, shifts progressively upward across the same series despite a majority contribution of $C_\beta C_\beta$ stretching to this mode in OEP (Abe et al., 1978). The upshift of this band in OEC has previously been attributed to "repulsive" mixing with the ν_{11} (B_{1g}) mode (Ozaki et al., 1986a), but because of the axis shift in the isobacteriochlorin system, mixing of A_{1g} and B_{1g} modes in OEiBC is not anticipated. An increase in the core-size sensitivity of this band was noted for OEC (Ozaki et al., 1986a); the same appears to be the case for siroheme (vide infra), indicating a larger contribution of the $C_\alpha C_m$ stretching coordinate to this mode in the reduced ring species. Indeed, we note from Table I that, with two exceptions, the frequencies of all the μ-oxo Fe^{III} dimer high-frequency modes increase from

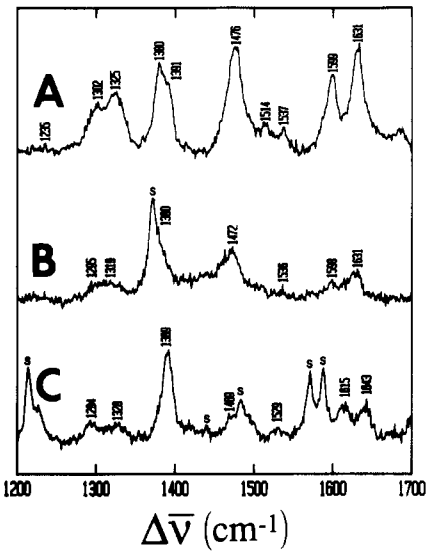

FIGURE 6: Room temperature RR spectra of siroheme extracted from SiR-HP. (A) Siroheme in acetone-d_6/HCl. To a 25-μL sample of purified SiR-HP^0 (603 μM) in standard buffer was added 300 μL of ice-cold acetone-d_6 containing 1% (v/v) concentrated HCl. The sample was incubated for 10 min on ice and then was centrifuged to remove precipitated protein. The supernatant was transferred into a 5-mm-o.d. NMR tube, and optical and RR spectra were obtained without delay (optical λ_{max} = 516, 542, 592, 702 nm). (B) Siroheme in CH_3CN/HCl. Prepared as in (A), but CH_3CN containing 1% (v/v) HCl was used as the extraction solvent. (C) Siroheme in pyridine. Sample was prepared by extraction of SiR-HP into acetone/HCl, followed by chromatography in pyridine on Sephadex LH-20 (Siegel et al., 1973) and concentration by evaporation to approximately 0.2 mM. A sloping background in the raw data due to fluorescent impurities was corrected by subtraction of a linear ramp from the raw data. "S" designates peaks due to solvent bands. Instrumental conditions (Spex 1402): power, 70 mW; slit, 7 cm^{-1}; scan increment, 1 cm^{-1}; acquisition time, 2 s/point (siroheme), 4 s/point (HP^0), 6 s/point (OEiBC).

OEP to OEC to OEiBC. Considering the decreased aromaticity (Abraham et al., 1987) and reduced pyrrole bond order of the hydroporphyrins, this result was surprising, but the relationship is identical with that previously observed (Ozaki et al., 1986b) in a comparison of iron OEP and OEC monomer complexes with a variety of axial ligands.

In the 1370–1400-cm^{-1} region where ν_4 (A_{1g}), the porphyrin oxidation state marker band, dominates the OEP RR spectra with Soret-band excitation, both OEC and OEiBC show three prominent bands. The lowest frequency band of the trio, at ~1372 cm^{-1}, is very weak in OEC and OEiBC. The OEC and OEiBC spectra show 1397-cm^{-1} bands that are depolarized and polarized, respectively, as expected for a B_{2g}-derived mode (ν_{29}). The middle band at ~1383 cm^{-1} in OEC is seen as a shoulder, and its frequency and polarization are difficult to determine accurately. It should be depolarized for both OEC and OEiBC to be assigned to ν_{20} (A_{2g}). However, the band at 1384 cm^{-1} in OEiBC is strong and no doubt polarized, making assignment as a correlate of ν_4 more plausible. In OEC others (Ozaki et al., 1986a) have assigned this band as an analogue of ν_{12} (B_{1g}), but the ν_{12} mode, which is undetectable in the OEP spectrum reported here, is expected to lie well below ν_4 (Abe et al., 1978).

Hemoprotein vs. Extracted Siroheme. In Figure 6 are shown RR spectra of extracted siroheme in a variety of solvents. In Figure 6A, the siroheme is in acetone-d_6/HCl solution and is therefore likely present as the chloro–Fe^{III} complex. This species as well as [Fe(OEiBC)]$_2$O are expected to be five-coordinate high-spin complexes (Scheidt & Gouterman, 1983). For porphyrins, the RR frequencies are known to be essentially the same for μ-oxo– and chloro–Fe^{III} complexes (Choi et al., 1982). The siroheme and [Fe(OEiBC)]$_2$O spectra show a generally similar band distribution, although there are downshifts in the siroheme bands averaging 7 cm^{-1} relative to the analogous [Fe(OEiBC)]$_2$O modes (see Figure 5). Because the altered peripheral substituents (refer to Figure 1) might have some effect, the significance of these modest frequency shifts is uncertain. The position of the band correlated to the porphyrin ν_3 mode [1502 cm^{-1} in [Fe(OEiBC)]$_2$O] cannot be determined for siroheme, which shows a broad band at ~1478 cm^{-1} that probably contains contributions from multiple bands. The remaining bands are quite comparable for the two complexes. It is concluded from this comparison that OEiBC is an adequate model for siroheme.

Larger differences are seen when SiR-HP^0 is compared with siroheme or [Fe(OEiBC)]$_2$O. There are both frequency shifts and intensity alterations. The two highest frequency modes, correlated with ν_{10} and ν_2, shift down significantly (15 and 11 cm^{-1}, respectively) relative to [Fe(OEiBC)]$_2$O. At the same time ν_3 (1488 cm^{-1}) and bands at 1280 and 1249 cm^{-1} all become more prominent in SiR-HP^0 [the latter two can hardly be seen for siroheme or [Fe(OEiBC)]$_2$O), while the 1397-cm^{-1}, ν_{29} band disappears in the protein (although it is prominent with Q-band excitation; see Figure 3)]. Alterations in the enhancement pattern are associated with electronic effects in the excited or ground states, while the frequency shifts imply structural changes in the siroheme ground state induced by binding to the protein. Three possible mechanisms are considered for the frequency shifts. (a) Ring deformations: Hydroporphyrin ring systems display enhanced conformational flexibility relative to porphyrins, as manifested in their tendency to undergo S_4 ruffling distortion (Kratky et al., 1985), which has been shown in Ni(OEP) (Spaulding et al., 1975) to significantly lower the frequency of the in-plane ring vibrational modes. Pyrrole tilt angles as large or larger than that observed in the ruffled form of Ni(OEP) are observed in a number of metalloisobacteriochlorin crystal structures (Suh et al., 1984; Strauss et al., 1983); on the basis of the electron density map of the active site it has been concluded (McRee et al., 1986) that the siroheme in SiR-HP is definitely ruffled. (b) Fe_4S_4 cluster–siroheme interaction: Transfer of charge from the cluster to the siroheme, as might be anticipated on the basis of structural and mechanistic considerations, would be expected to decrease the siroheme ring mode frequencies by populating ring π^* orbitals. This hypothesis is weakened, however, by the observation (next section) that the siroheme frequencies of the CO adduct are independent of the Fe_4S_4 oxidation level. (c) Altered axial coordination: Binding of a sixth ligand to high-spin siroheme would be expected to lower ν_{10}, ν_2, and ν_3 via the resulting expansion of the core (Teraoka & Kitagawa, 1980). The ligation state of the siroheme in SiR-HP^0 is not known with certainty. However, EPR and ENDOR measurements (Cline et al., 1985) have indicated the absence of nitrogenous ligands, or of a bound water molecule, and the X-ray structure (McRee et al., 1986) does not appear to show significant electron density on the distal side of the siroheme Fe atom in SiR-HP^0. Thus, a five-coordinate siroheme seems likely in SiR-HP^0, although the issue cannot be fully settled until an atomic level structure is available. At present none of these three possibilities can be ruled out, but ring distortion presents the fewest difficulties.

Figure 6B shows the RR spectrum of siroheme in acetonitrile. The band positions are similar to those in acetone/HCl solution, indicating the presence of high-spin iron. This is as expected, on the basis of the optical spectral similarity of these

Table II: Vibrational Frequencies (cm^{-1}) for Heme Modes at 77 K

HP^0	HP^{1-}–CO	HP^{2-}–CO	HP^0–CN^- [a]	HP^{2-}–CN^-	HP^{1-}–NO/Ox [a,b]	HP^{1-}–NO	HP^{2-}/SO_3^{2-}/Ox [c,d]	HP^{2-}/SO_3^{2-} [d]	mode correlation
1626	1644	1647	1644	1644	1646	1649	1643	1643	ν_{10}
1600	1618	1621	1629	1621	1629	1622	1623	1619	ν_2
1585	1601	1600	1593	1595	1603	1601			ν_{19}
1540	1553	1555		1554		1555			ν_{38}
1528	1546	1546		1547		1547			ν_{38}
	1514	sh [e]	1517	1510	1518				ν_{11}
1489	1501	1504		1493		1509	~1496	~1496	ν_3
1472	1488	1488	1479	1483		1490	1483	1481	ν_{28}
	1476	1475		1470	1476	1479			
				1456	1451	1456			
	1416	1416	1420	1417	1418	1418			
1391	1395	1395	1398	1393	1398	1397	1394	~1395	ν_{29}
1378	1388	1391		1388		1385	1383	1383	ν_1
	1340	1341		1338					
1325	1325	1326	1322	1325	1323	1327	1320	1318	ν_{21}
1316				1314		1319			
1303	1302	1306	1300	1305	1305	1303	1294	1296	
1282	1285	1287	1282	1283	1285	1287	1277	1277	
1250	1250	1252	1245	1251	1247	1252			
1220	1222	1220	1227	1223	1223	1221			ν_{13}

[a] Data obtained from Q-band-excited spectra. [b] Ferricyanide-treated form of HP^{1-}–NO (see legend to Figure 9). [c] HP^{2-}/SO_3^{2-} (see legend to Figure 9) treated with 2.2 mol of ferricyanide/mol of enzyme. [d] Room temperature spectra. [e] Shoulder.

two preparations (data not shown). By contrast, the RR spectrum of siroheme in pyridine solution (Figure 6C), for which a hemochromogen-type optical spectrum characteristic of low-spin iron is observed (Siegel et al., 1973), displays upshifts in the highest frequency bands to 1643 and 1615 cm^{-1}. Smaller upshifts of most of the other bands relative to the high-spin ferric siroheme preparations are also seen. Such upshifts upon generation of a low-spin adduct are entirely consistent with the well-established structural sensitivity of iron porphyrins and chlorins and are also characteristic of the behavior of siroheme in SiR-HP (vide infra).

Low-Spin SiR-HP Adducts. The interaction of SiR-HP^0 with potential siroheme ligands is extremely sluggish, but many complexes are formed readily upon reduction of the protein (Rueger & Siegel, 1976; Siegel et al., 1982). Once an exogenous ligand is bound to the reduced enzyme, oxidation is possible to ligated SiR-HP^{1-}, in which the Fe_4S_4 is oxidized but the siroheme remains reduced, or to ligated SiR-HP^0, in which both Fe_4S_4 and the siroheme Fe are oxidized. When CO is bound, reoxidation stops at SiR-HP^{1-}–CO, since CO only binds to Fe^{II} siroheme. Oxidation of the cyanide complex, however, proceeds to SiR-HP^0-CN^- (Janick & Siegel, 1983). When SiR-HP^{2-} reacts with NO_2^-, which is a substrate for the enzyme, the species left once the reductant is exhausted is SiR-HP^{1-}–NO, the nitrosyl–Fe^{II} siroheme adduct with oxidized Fe_4S_4 (Janick et al., 1983). This can be further oxidized to an incompletely characterized product, probably a mixture of species.

RR spectra of the CO, CN^-, and NO complexes of SiR-HP are shown in Figure 7, and their frequencies are compared with those of SiR-HP^0 in Table II. The most notable aspect of these data are the large upshifts, relative to SiR-HP^0, ~10–20 cm^{-1}, in all of the modes above 1472 cm^{-1}. These upshifts are entirely consistent with those seen for iron porphyrins upon conversion from high- to low-spin complexes (Spiro & Li, 1988). The higher frequencies for the low-spin complexes are expected because of their smaller core sizes due to the emptying of the in-plane antibonding $d_{x^2-y^2}$ orbital. The complexes in Table I (with the exception of the incompletely characterized ferricyanide-treated nitrosyl complex) are known to be low spin from EPR and Mössbauer studies (Janick & Siegel, 1982, 1983; Janick et al., 1983). Thus, the siroheme skeletal vibrational frequencies appear to show the same sensitivity to spin state, presumably via the core-size sensitivity, as do the porphyrin modes. Furthermore, except for the unexpectedly large upshift of the ν_2 mode already noted, the degree of the upshift for each of the siroheme high-frequency bands upon generation of the low-spin species corresponds quite well to the relative sensitivities established for the corresponding bands in porphyrin systems (Ozaki et al., 1986a; Parthasarathi et al., 1987).

The porphyrin frequencies are also influenced by the Fe oxidation state (Spiro & Li, 1988). This effect is associated with back donation of Fe^{II} $d\pi$ electrons to the porphyrin e_g^* orbitals that depresses the frequencies of several of the high-frequency skeletal modes. (In the case of high-spin Fe^{II} the effect is believed to be associated with porphyrin doming, rather than back donation.) The back-donation effect is diminished when Fe^{II} is bound to π acid ligands that compete with the porphyrin e_g^* orbital for the Fe^{II} $d\pi$ electrons. This is no doubt the reason that the frequencies of the Fe^{II}–CO and –NO complexes in SiR-HP (see Table I) are about as high as those shown by the Fe^{III}–CN^- complex in SiR-HP^0–CN^-. What is more surprising is that the Fe^{II}–CN^- frequencies in SiR-HP^{2-}–CN^- are also nearly as high; CN^- is a much weaker π acid than CO or NO, and the porphyrin frequencies of the cyanide adduct of Fe^{II} horseradish peroxidase are distinctly lower than those of the Fe^{III} adduct (Rakhit & Spiro, 1974). In an accompanying paper, evidence is presented indicating that H-bonding of bound ligands is a likely feature of the sulfite reductase active site; such an interaction could enhance the π-acceptor ability of the cyanide ligand, accounting in part for the unusually high ring mode frequencies.

In Fe porphyrins, the effect of the oxidation state is particularly clear-cut on the skeletal mode ν_4 (Spiro, 1983), which shows only a weak core-size, and therefore spin-state, dependence (Parthasarathi et al., 1987). The frequency is ~15 cm^{-1} lower for Fe^{II} (~1355 cm^{-1}) than for Fe^{III} (~1370 cm^{-1}) hemes. The oxidation-state influence on ν_4 is smaller in chlorins (Ozaki et al., 1986a) than in porphyrins, however, and in siroheme there does not appear to be a reliable correlation. Table I shows that the low-spin complexes, all of which are effectively Fe^{III} due to the π acid ligands, exhibit ~10-cm^{-1} upshifts in the band that we consider analogous to ν_4 relative

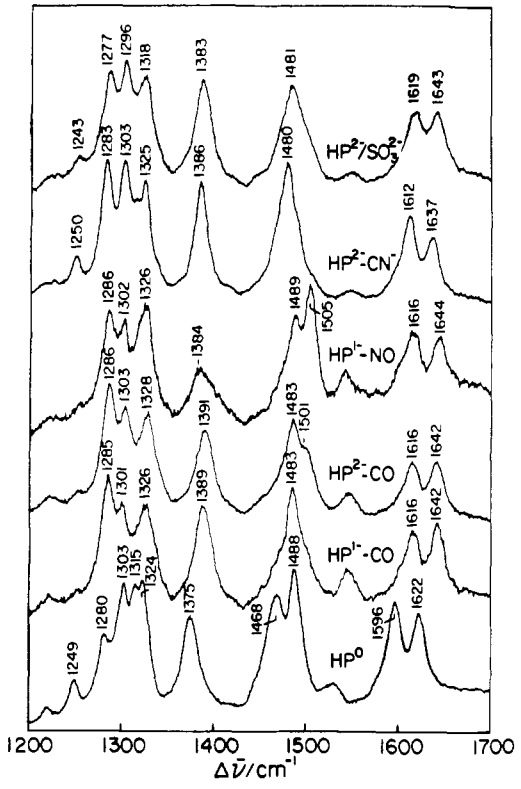

FIGURE 7: Room temperature RR spectra of various low-spin adducts of SiR-HP obtained with Soret (406.7 nm) excitation. HP^0: SiR-HP (203 μM) as isolated, in standard buffer. HP^{2-}–CO: To degassed SiR-HP (120 μL, 203 μM) in standard buffer contained in a standard 5-mm NMR tube was anaerobically added 10 μL of 17 mM Cr^{II}(EDTA) (7-fold molar excess), and the tube was flushed with CO gas (optical λ_{max} = ~404, 606 nm). HP^{1-}–CO: 100 μL of air was injected into the tube containing the previous sample, which was shaken and incubated briefly on ice (optical λ_{max} = ~404, 600 nm). HP^{1-}–NO: To degassed SiR-HP (120 μL, 203 μM) in standard buffer was anaerobically added 10 μL of 18 mM Cr^{II}(EDTA) (7-fold molar excess), followed by 10 μL of 0.1 M $NaNO_2$ (41-fold molar excess, 7.1 mM final NO_2^- concentration) (optical λ_{max} = 398, 596 nm). HP^{2-}–CN: To degassed SiR-HP (120 μL, 203 μM) in standard buffer was anaerobically added 10 μL of 18 mM Cr^{II}(EDTA) (7-fold molar excess), followed by 5 μL of 0.25 M KCN neutralized with HCl (50-fold molar excess, final $[CN^-]$ = 9 mM) (optical I_{max} = 402, 544 nm). HP^{2-}/SO_3^{2-}: To degassed SiR-HP (120 μL, 203 μM) in standard buffer was anaerobically added 10 μL of 18 mM Cr^{II}(EDTA) (7-fold molar excess), followed by 5 μL of 0.1 M Na_2SO_3 in standard buffer (20-fold molar excess, final $[SO_3^{2-}]$ = 3.7 mM) (optical λ_{max} = ~395, 588 nm). Instrumental conditions (Spex 1877): power, 25 mW ($SiR\text{-}HP^{2-}$–CN^-), 75 mW ($SiR\text{-}HP^{1-}$–CO, –NO, $SiR\text{-}HP^{2-}/SO_3^{2-}$), 100 mW ($SiR\text{-}HP^{2-}$–CO); slit, 150 μm; integration time, 150 s ($SiR\text{-}HP^{2-}$–CN^-), 300 s (others).

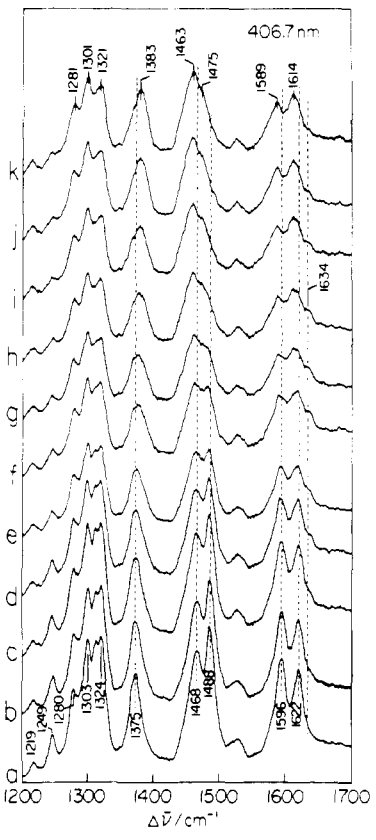

FIGURE 8: Sequential reduction of SiR-HP. The RR spectrum of the fully oxidized protein is designated a. To a deoxygenated 120-μL sample of $SiR\text{-}HP^0$ at 203 μM in standard buffer at room temperature contained in a 5-mm-o.d. NMR tube sealed with a rubber septum were added successive 1.5-μL aliquots of Cr^{II}(EDTA) reductant solution (total [Cr] = 7.3 mM). After each addition the optical spectrum was obtained to monitor reduction level, and then the RR spectrum was collected by using excitation at 406.7 nm. The optical spectrum was obtained again to check for reoxidation before addition of the next aliquot of reductant; no significant change in the optical spectra was observed. The fully reduced spectrum is designated k. Instrumental conditions (Spex 1877): slit, 150 μm; integration time, 300 s.

to $SiR\text{-}HP^0$, which contains high-spin Fe^{III}. Upon reduction of $SiR\text{-}HP^0$ the band appears to shift up rather than down, as discussed in the next section.

The RR spectra of $SiR\text{-}HP^{2-}$–CO with $SiR\text{-}HP^{1-}$–CO are compared in Figure 7 and in Table II. In both complexes the siroheme is in the low-spin ferrous state, the only difference being the reduction state of the Fe_4S_4 cluster. Although the spectra are quite similar, the former species shows significantly augmented intensity for the 1501-cm^{-1} ν_3 band. This intensity change is attributable to the electronic effect of reduction of the coupled iron–sulfur cluster in $SiR\text{-}HP^{2-}$ species. On the other hand, the siroheme frequencies are little affected by the Fe_4S_4 oxidation level. This observation weighs against the possibility of significant $Fe_4S_4 \rightarrow$ siroheme charge transfer (see preceding section), at least in the CO-bound form.

Sulfite is the natural substrate of the enzyme, and its addition to $SiR\text{-}HP^{2-}$ leads to formation of an EPR-silent species (Janick & Siegel, 1983). The composition of this intermediate is unknown, but the addition of excess reductant leads to turnover and sulfide production. Oxidation of the intermediate produces another EPR-silent air-stable species. Magnetic susceptibility (Day et al., 1988) and Mössbauer data (Janick et al., 1983) indicate that the latter complex contains low-spin ferriheme and an oxidized Fe_4S_4 cluster. Comparison of the RR spectra of the intermediate (Figure 7) and its oxidation product (see Table II) shows that both contain low-spin siroheme since ν_{10} and ν_2 are at ~1640 and ~1620 cm^{-1}, respectively, in each of the two complexes.

Reduced SiR-HP. Figure 8 shows room temperature RR spectra for a solution of SiR-HP incrementally reduced by the addition of aliquots of Cr^{II}(EDTA). The absorption spectra were essentially identical with those produced by deazaflavin photoreduction (Janick & Siegel, 1982) (an inapplicable procedure for RR studies because of the interference from deazaflavin fluorescence). It can be seen that significant band frequency shifts occur in the course of the reduction. In particular, we call attention to the two highest frequency bands, assigned as the analogues of ν_{10} and ν_2. These shift downward from 1622 and 1596 cm^{-1} in $SiR\text{-}HP^0$ to 1614 and 1589 cm^{-1} in the fully reduced form. These downshifts are similar to those observed for ν_{10} and ν_2 in iron protoporphyrin when a high-spin Fe^{III} complex is converted to a high-spin Fe^{II} complex. Accordingly, $SiR\text{-}HP^{2-}$ in room temperature solution is inferred to contain a high-spin Fe^{II} siroheme. Recently, the

RR spectrum of reduced nitrite reductase (Ondrias et al., 1985) was interpreted as indicating the presence of low-spin siroheme; this result, however, is likely to be an artifact of the use of dithionite as a reducing agent. The dithionite reaction product is sulfite, which is a substrate for nitrite reductase as well as sulfite reductase. Consequently, a sulfite complex can be formed, with a RR spectrum of low-spin character (see Table II).

As noted in the previous section, ν_4 does not follow the porphyrin pattern, its frequency apparently shifting up upon reduction from 1375 to 1383 cm^{-1}. Ozaki et al. (1986a) observed for iron chlorins that the downshift of ν_4 on reduction was significantly smaller than for iron porphyrins; thus, the frank reversal of the direction of the shift in siroheme could represent a continuation of this trend with increasing ring reduction. Those authors speculated that the smaller shift was due to decreased π back donation from ferrous ion in chlorins compared with porphyrins; this explanation is inadequate to account for an actual reversal of the shift in siroheme. The ν_4 band in porphyrins differs from other prominent high-frequency modes in that its chief contribution is $C_\alpha N$ bond motion. Interestingly, examination of published crystal structures reveals an obvious pattern of long-short-long-short bond length alteration extending over adjacent $C_\alpha NC_\alpha$ units of isobacteriochlorins. The same pattern occurs in chlorins, where it instead affects the bond lengths in adjacent pairs of $C_\alpha C_m C_\alpha$ units. The localization of $C_\alpha C_m$ vibrations that appeared in normal mode calculations on chlorin (Boldt et al., 1987) was rationalized as the direct kinematic result of this bond-length alternation. It cannot be excluded therefore that the anomalous behavior of ν_4 in siroheme results, mutatis mutandis, from mode localization affecting $C_\alpha N$ motion in the isobacteriochlorin skeleton. Finally, it is possible that the apparent upshift merely results from a redistribution of intensity among the closely spaced modes found in this region.

The midpoint potentials of the siroheme and Fe_4S_4 cluster in SiR-HP are spaced sufficiently closely that solutions at intermediate reduction levels which contain the major one-electron species (siroheme reduced, cluster oxidized) inevitably include admixtures of oxidized or fully reduced SiR-HP (Janick & Siegel, 1982). Nevertheless, examination of the spectra (Figure 8) representing intermediate stages in the reduction of SiR-HP reveals features that are not merely superpositions of initial and final spectra. A key finding is the appearance of a band at 1634 cm^{-1} that is not present in either SiR-HP^0 or SiR-HP^{2-}; this band is seen most clearly upon addition of approximately one electron (as determined by examination of the accompanying optical spectra) when the SiR-HP^{1-} concentration is maximal (Figure 8g). The highest frequency band in the SiR-HP spectrum is the analogue of ν_{10}, and it is apparent that this band shifts *up* in SiR-HP^{1-}, despite the conversion of Fe^{III} to Fe^{II} siroheme. (An upshift is also inferred for ν_2, but the precise position is obscured by overlapping bands in the mixture.) These upshifts in the solution RR spectra of SiR-HP^{1-} are suggestive of low- or intermediate-spin ferrous siroheme formation. Intermediate-spin siroheme is consistent with the upshifted RR bands, since in this spin state the $d_{x^2-y^2}$ orbital is empty and the macrocycle core is contracted; it has been demonstrated for Fe^{II} porphyrin that the intermediate-spin skeletal mode frequencies are as high as the low-spin frequencies (Spiro & Burke, 1976). Mössbauer measurements have indicated that the siroheme Fe^{II} is intermediate spin (or possibly high spin) in SiR-HP^{1-} in the frozen state (Christner et al., 1981). Thus, the simplest explanation for the RR and Mössbauer data, taken together, is an intermediate-spin state for the siroheme Fe^{II} in SiR-HP^{1-}. (We have been unsuccessful to date in preparing well-defined samples of SiR-HP^{1-} in the frozen state suitable for RR spectroscopy. Thus, a transition from low-spin ferrous siroheme to intermediate-spin (or high-spin) ferrous siroheme induced by freezing of SiR-HP^{1-} cannot be excluded by the present data.)

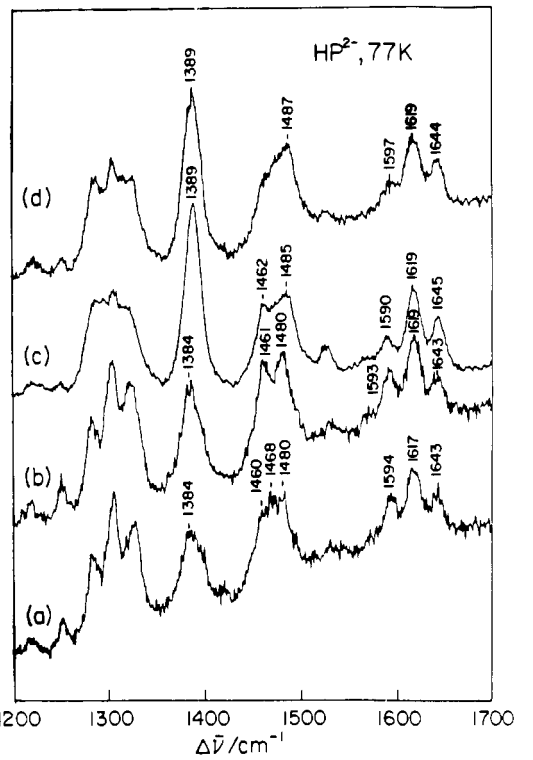

FIGURE 9: RR spectra of fully reduced SiR-HP in the frozen state (77 K) obtained with B-band (406.7 nm) excitation. (a) Standard buffer, no additions, final [SiR-HP] = 196 μM, reduced with a 14-fold excess of Cr^{II}(EDTA) prepared without chloride. (b) Standard buffer plus 0.025 M guanidinium sulfate, final [SiR-HP] = 162 μM, reduced with a 14-fold excess of Cr^{II}(EDTA). (c) Standard buffer plus 0.1 M guanidinium chloride, final [SiR-HP] = 222 μM, reduced with a 9-fold excess of Cr^{II}(EDTA). (d) Standard buffer plus 0.15 M guanidinium sulfate, final [SiR-HP] = 162 μM, reduced with 14-fold excess Cr^{II}(EDTA). Instrumental conditions (Spex 1402): slit, 7 cm^{-1}; scan increment, 1 cm^{-1}; acquisition time, 2 s/point.

The RR spectrum of SiR-HP^{2-} was altered dramatically when the solution was frozen (Figure 9). A significant portion of the intensity in the two highest frequency bands at 1596 and 1614 cm^{-1} shifted upward to ~1615 and 1643 cm^{-1}, indicative of a contribution from a low- or intermediate-spin spiroheme species. (The possibility that this band was due to reoxidation to SiR-HP^{1-} during sample transfer was excluded by monitoring the optical spectrum of the sample in situ prior to freezing.) This result may throw light on the complexity of the EPR and Mössbauer spectra of SiR-HP^{2-}, which were necessarily obtained in the frozen state. The EPR spectrum of the two-electron-reduced species (SiR-HP^{2-}) reveals multiple signals (Janick & Siegel, 1983) that fall into two classes. One class of EPR signals (g = 5 type) arises from high-spin (S = 2) ferrous siroheme antiferromagnetically coupled to the reduced cluster, while the other (g = 2.29 type) may represent intermediate-spin ferrous siroheme similarly coupled to the cluster. The g = 2.29 type constitute the majority species in frozen solutions of enzyme reduced in standard buffer. The RR spectral findings of spectroscopic heterogeneity are entirely consistent with these results; however, the room temperature spectra imply that any intermediate- or low-spin siroheme contribution arises as a consequence of freezing and that in

liquid solution SiR-HP^{2-} contains only high-spin ferrous siroheme. The absence of any change in the ratio of these two signals over the temperature range 77–244 K suggests that this effect is a macroscopic physical effect of freezing, rather than the manifestation of a spin-state equilibrium. On the other hand, EPR investigations (Janick & Siegel, 1983) have established that in the presence of agents such as guanidinium or halide ions the ratio of the two types of EPR-detectable species is significantly altered. Little change in the relative intensities of the upshifted bands was noted in the RR spectra of frozen SiR-HP^{2-} obtained in the presence of perturbing agents (Figure 9b–d); it would be incorrect therefore to infer an identity between the species defined by these two spectroscopic methods.

Conclusions. Resonance Raman features of the siroheme moiety of SiR-HP are in keeping with those expected for a tetrapyrrole macrocycle of approximate C_{2v} symmetry and include an increase in the total number of bands and in the number of polarized bands, the presence of new, strongly enhanced polarized bands in the porphyrin oxidation-state marker region, generally somewhat weaker enhancement than in typical porphyrin spectra but predominance of polarized bands with both Soret and Q-band excitation. While the foregoing features are familiar from chlorin spectra, the polarization properties of siroheme and of an OEiBC model clearly reflect the effect of the altered orientation of the major isobacteriochlorin symmetry axis relative to that of chlorin. Anomalous polarization of the highest frequency, strongly enhancing ring mode near 1630 cm^{-1}, which we infer to be the analogue of the porphyrin ν_{10} vibration, appears to be a diagnostic feature of isobacteriochlorin spectra. The spin-state sensitivity of the high-frequency modes of siroheme is similar to that observed in porphyrins and chlorins; however, the response to oxidation-state changes of the band which we correlate with the porphyrin oxidation-state marker (ν_4) is anomalous. On the basis of these structural sensitivities we infer the presence of low-spin siroheme in the product of fully reduced SiR-HP with its substrate, sulfite. In partially reduced solutions of free SiR-HP there is evidence of a species with upshifted ring mode frequencies, consistent with the presence of intermediate-spin ferroheme in the one-electron-reduced adduct of the enzyme, as suggested by earlier Mössbauer studies. In the fully reduced enzyme, freezing appears to generate a mixture of high- and intermediate- or low-spin species, but in liquid solution, the fully reduced enzyme contains high-spin ferroheme.

Registry No. $[Fe(OEP)]_2O$, 39393-88-9; $[Fe(OEC)]_2O$, 54643-20-8; $[Fe(OEi)BC)]_2O$, 78325-75-4; NADPH–sulfite reductase, 9029-35-0; siroheme, 52553-42-1.

REFERENCES

Abe, M., Kitagawa, T., & Kyogoku, Y. (1978) *J. Chem. Phys. 69*, 4526–4534.

Abraham, R. J., Medforth, C. J., Smith, K. M., Goff, D. A., & Simpson, D. J. (1987) *J. Am. Chem. Soc. 109*, 4786–4791.

Andersson, L. A., Loehr, T. M., Lim, A. R., & Mauk, A. G. (1984) *J. Biol. Chem. 259*, 15340–15349.

Andersson, L. A., Loehr, T. M., Chang, C. K., & Mauk, A. G. (1985) *J. Am. Chem. Soc. 107*, 182–191.

Andersson, L. A., Loehr, T. M., Sotiriou, C., Wu, W., & Chang, C. K. (1986) *J. Am. Chem. Soc. 108*, 2908–2916.

Babcock, G. T., Ingle, R. T., Oertling, W. A., Davis, J. C., Averill, B. A., Hulse, C. L., Stufkens, D. J., Bolscher, B. G. J. M., & Wever, R. (1985) *Biochim. Biophys. Acta 828*, 58–66.

Boldt, N. J., Donohoe, R. J., Birge, R. R., & Bocian, D. F. (1987) *J. Am. Chem. Soc. 109*, 2284–2298.

Choi, S., Spiro, T. G., Langry, K. C., Smith, K. M., Budd, D. L., & La Mar, G. N. (1982) *J. Am. Chem. Soc. 104*, 4345–4351.

Christner, J. A., Münck, E., Janick, P. A., & Siegel, L. M. (1981) *J. Biol. Chem. 256*, 2098–2101.

Christner, J. A., Münck, E., Janick, P. A., & Siegel, L. M. (1983) *J. Biol. Chem. 258*, 11147–11156.

Christner, J. A., Münck, E., Kent, T. A., Janick, P. A., Salerno, J. C., & Siegel, L. M. (1984) *J. Am. Chem. Soc. 106*, 6786–6794.

Cline, J. F., Janick, P. J., Siegel, L. M., & Hoffman, B. M. (1985) *Biochemistry 24*, 7942–7947.

Cotton, T. M., Timkovich, R., & Cork, M. S. (1981) *FEBS Lett. 133*, 39–44.

Czernuszewicz, R. S., & Johnson, M. K. (1983) *Appl. Spectrosc. 37*, 297–298.

Day, E. P., Peterson, J., Bonvoisin, J. J., Young, L. J., Wilkerson, J. O., & Siegel, L. M. (1988) *Biochemistry 27*, 2126–2132.

den Boef, G., de Johng, W. J., Krijn, G. C., & Poppe, H. (1960) *Anal. Chim. Acta 23*, 557–564.

Gouterman, M. J. (1961) *Mol. Spectrosc. 6*, 138–163.

Henderson, R. A., & Sykes, A. G. (1980) *Inorg. Chem. 19*, 3103–3105.

Hildebrandt, P., & Spiro, T. G. (1988) *J. Phys. Chem. 92*, 3355–3360.

Janick, P. A., & Siegel, L. M. (1982) *Biochemistry 21*, 3538–3547.

Janick, P. A., & Siegel, L. M. (1983) *Biochemistry 22*, 504–515.

Janick, P. A., Rueger, D. C., Krueger, R. J., Barber, M. J., & Siegel, L. M. (1983) *Biochemistry 22*, 396–408.

Kitagawa, T., & Ozaki, Y. (1987) *Struct. Bonding (Berlin) 64*, 1–70.

Kratky, C., Waditschatka, R., Angst, C., Johansen, J. E., Plaquevent, J. C., Schreiber, J., & Eschenmoser, A. (1985) *Helv. Chim. Acta 68*, 1312–1337.

Massey, V., & Hemmerich, P. (1978) *Biochemistry 17*, 9–17.

McRee, D. E., Richardson, D. C., Richardson, J. S., & Siegel, L. M. (1986) *J. Biol. Chem. 261*, 10277–10281.

Murphy, M. J., Siegel, L. M., Kamin, H., & Rosenthal, D. (1973) *J. Biol. Chem. 248*, 2801–2814.

Ondrias, M. R., Rousseau, D. L., Muhoberac, B. B., & Wharton, D. C. (1982) *FEBS Lett. 138*, 239–244.

Ondrias, M. R., Carson, S. D., Hirasawa, M., & Knaff, D. B. (1985) *Biochim. Biophys. Acta 830*, 159–163.

Ozaki, Y., Kitagawa, T., & Ogoshi, H. (1979) *Inorg. Chem. 18*, 1772–1776.

Ozaki, Y., Iriyama, K., Ogoshi, H., Ochiai, T., & Kitagawa, T. (1986a) *J. Phys. Chem. 90*, 6105–6112.

Ozaki, Y., Iriyama, K., Ogoshi, H., Ochiai, T., & Kitagawa, T. (1986b) *J. Phys. Chem. 90*, 6113–6118.

Parthasarathi, N., Hanson, C., Yamaguchi, S., & Spiro, T. G. (1987) *J. Am. Chem. Soc. 109*, 3865–3871.

Rakhit, G., & Spiro, T. G. (1974) *Biochemistry 13*, 5317–5323.

Rueger, D. C., & Siegel, L. M. (1976) in *Flavins and Flavoproteins* (Singer, T. P., Ed.) pp 610–620, Elsevier, New York.

Scheidt, W. R., & Gouterman, M. (1983) in *Iron Porphyrins* (Lever, A. B. P., & Gray, H. B., Eds.) Part I, pp 89–140, Addison-Wesley, Reading, MA.

Shelnutt, J. A. (1987) *J. Am. Chem. Soc. 109*, 4169–4173.

Sibbett, S. S., & Hurst, J. K. (1984) *Biochemistry 23*, 3007–3013.
Siegel, L. M., & Davis, P. S. (1974) *J. Biol. Chem. 249*, 1587–1598.
Siegel, L. M., Murphy, M. J., & Kamin, H. (1973) *J. Biol. Chem. 248*, 251–264.
Siegel, L. M., Rueger, D. C., Barber, M. J., Krueger, R. J., Orme-Johnson, N. R., & Orme-Johnson, W. H. (1982) *J. Biol. Chem. 257*, 6343–6350.
Spaulding, L. D., Chang, C. C., Yu, N.-T., & Felton, R. H. (1975) *J. Am. Chem. Soc. 97*, 2517–2525.
Spiro, T. G. (1983) in *Iron Porphyrins* (Lever, A. B. P., & Gray, H. B., Eds.) Part II, pp 89–160, Addison-Wesley, Reading, MA.
Spiro, T. G. (1985) *Adv. Protein Chem. 37*, 11–154.
Spiro, T. G., & Burke, J. M. (1976) *J. Am. Chem. Soc. 98*, 5482–5489.
Spiro, T. G., & Li, X.-Y. (1988) in *Biological Applications of Raman Spectroscopy* (Spiro, T. G., Ed.) Vol. 3, pp 1–37, Wiley-Interscience, New York.
Spiro, T. G., Czernuszewicz, R. S., & Han, S. (1988) in *Biological Applications of Raman Spectroscopy* (Spiro, T. G., Ed.) Vol. 3, pp 523–553, Wiley-Interscience, New York.
Stoltzenberg, A. M., Strauss, S. H., & Holm, R. H. (1981) *J. Am. Chem. Soc. 103*, 4763–4778.
Strauss, S. H., Silver, M. E., & Ibers, J. A. (1983) *J. Am. Chem. Soc. 105*, 4108–4109.
Suh, M. P., Swepston, P. N., & Ibers, J. A. (1984) *J. Am. Chem. Soc. 106*, 5164–5171.
Teraoka, J., & Kitagawa, T. (1980) *J. Phys. Chem. 84*, 1928–1935.
Tsai, H., Sweeney, W. V., & Coyle, C. L. (1985) *Inorg. Chem. 24*, 2796–2798.

Resonance Raman Studies of *Escherichia coli* Sulfite Reductase Hemoprotein. 2. Fe_4S_4 Cluster Vibrational Modes†

John F. Madden,‡ Sanghwa Han,§ Lewis M. Siegel,*,‡ and Thomas G. Spiro§
Department of Biochemistry, Duke University Medical Center and Veterans Administration Hospital, Durham, North Carolina 27705, and Department of Chemistry, Princeton University, Princeton, New Jersey 08540
Received November 4, 1988; Revised Manuscript Received March 14, 1989

ABSTRACT: Resonance Raman (RR) spectra from the hemoprotein subunit of *Escherichia coli* sulfite reductase (SiR-HP) are examined in the low-frequency (200–500 cm^{-1}) region where Fe–S stretching modes are expected. In spectra obtained with excitation in the siroheme Soret or Q bands, this region is dominated by siroheme modes. Modes assignable to the Fe_4S_4 cluster are selectively enhanced, however, with excitation at 488.0 or 457.9 nm. The assignments are confirmed by observation of the expected frequency shifts in SiR-HP extracted from *E. coli* grown on ^{34}S-labeled sulfate. The mode frequencies and isotopic shifts resemble those seen in RR spectra of other Fe_4S_4 proteins and analogues, but the breathing mode of the cluster at 342 cm^{-1} is higher than that observed in the other species. Spectra of various ligand complexes of SiR-HP reveal only slight sensitivity of the cluster terminal ligand modes to the presence of exogenous heme ligands, at variance with a model of ligand binding in a bridged mode between heme and cluster. Close examination of RR spectra obtained with siroheme Soret-band excitation reveals additional ^{34}S-sensitive features at 352 and 393 cm^{-1}. These may be attributed to a bridging thiolate ligand.

The active site of *Escherichia coli* sulfite reductase hemoprotein (SiR-HP) comprises an Fe_4S_4 cluster exchange coupled to a siroheme prosthetic group (Christner et al., 1981; Janick & Siegel, 1982, 1983; Siegel et al., 1982). A model of the active site has been proposed (Christner et al., 1984) in which one cluster Fe is covalently bridged to the siroheme Fe by an S atom of a cysteinyl ligand. The X-ray crystal structure (McRee et al., 1986) is consistent with this model; it shows the cluster to be closely apposed to the heme and reveals that one of the Fe_4S_4 cubane sulfur atoms is in van der Waals contact with the siroheme periphery. At the present level of resolution, however, the putative bridging thiolate itself is not clearly discernible.

Structurally, the Fe_4S_4 core in SiR-HP appears to conform closely to that observed in "typical" four-iron clusters. The electron density map of the cluster region in SiR-HP is well fit by an idealized Fe_4S_4 model derived from crystallographic data from previously characterized clusters (McRee et al., 1986). The SiR-HP cluster has been studied by magnetic spectroscopy in a variety of derivatives of the enzyme and does not appear to deviate significantly from representative Fe_4S_4 clusters in its internal electronic structure. Thus, the Mössbauer parameters, ΔE_Q and δ, of the cluster irons (Christner et al., 1981; Janick & Siegel, 1982, 1983) in both the oxidized (2+) and reduced (1+) states are essentially the same as those observed in other well-characterized Fe_4S_4 proteins such as *Bacillus stearothermophilus* ferredoxin (Münck & Kent, 1987). Upon reduction of CN^-- or CO-ligated SiR-HP the expected $g = 1.94$ EPR signal typical of Fe_4S_4 clusters in the 1+ state is observed (Janick & Siegel, 1982, 1983). On the other hand, the Mössbauer measurements of the magnetic coupling between the siroheme and the cluster irons in SiR-HP are markedly sensitive to the electronic state of the siroheme, and novel EPR signals are observed for the

† This work was supported by Grant GM 13498 (T.G.S.), Grant GM 31554 (S.H.S.), and Grant GM 32210 (L.M.S.) from the National Institutes of Health and by Project Grant 7875-01 from the Veterans Administration (L.M.S.). J.F.M. is a fellow of the Medical Scientist Training Program at Duke University.
‡ Duke University Medical Center and Veterans Administration Hospital.
§ Princeton University.

0006-2960/89/0428-5471$01.50/0